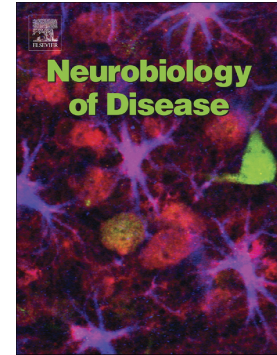


## Accepted Manuscript

A differentiating neural stem cell-derived astrocytic population mitigates the inflammatory effects of TNF- $\alpha$  and IL-6 in an iPSC-based blood-brain barrier model

Jennifer L. Mantle, Kelvin H. Lee



PII: S0969-9961(18)30356-5  
DOI: doi:[10.1016/j.nbd.2018.07.030](https://doi.org/10.1016/j.nbd.2018.07.030)  
Reference: YNBDI 4240  
To appear in: *Neurobiology of Disease*  
Received date: 4 August 2017  
Revised date: 6 June 2018  
Accepted date: 29 July 2018

Please cite this article as: Jennifer L. Mantle, Kelvin H. Lee , A differentiating neural stem cell-derived astrocytic population mitigates the inflammatory effects of TNF- $\alpha$  and IL-6 in an iPSC-based blood-brain barrier model. Ynbdi (2018), doi:[10.1016/j.nbd.2018.07.030](https://doi.org/10.1016/j.nbd.2018.07.030)

This is a PDF file of an unedited manuscript that has been accepted for publication. As a service to our customers we are providing this early version of the manuscript. The manuscript will undergo copyediting, typesetting, and review of the resulting proof before it is published in its final form. Please note that during the production process errors may be discovered which could affect the content, and all legal disclaimers that apply to the journal pertain.

# **A differentiating neural stem cell-derived astrocytic population mitigates the inflammatory effects of TNF- $\alpha$ and IL-6 in an iPSC-based blood-brain barrier model**

Jennifer L. Mantle and Kelvin H. Lee\*

## **\*Corresponding Author**

Kelvin H. Lee

Delaware Biotechnology Institute

15 Innovation Way

Newark, Delaware 19711

Phone: 302-831-4888

Email: [KHL@udel.edu](mailto:KHL@udel.edu)

## **Author Affiliations**

Department of Chemical and Biomolecular Engineering and Delaware Biotechnology Institute, University of Delaware, 15 Innovation Way, Newark, Delaware 19711, United States

## **Acknowledgements**

This work was funded in part by the National Science Foundation (Award Number 1144726). We wish to thank John Ruanos-Salguero for his assistance with neural stem cell culture and differentiation.

## **Conflict of Interest**

The authors declare no competing financial interests.

## ABSTRACT

Inflammation can be a risk factor for neurodegenerative diseases such as Alzheimer's disease (AD) and may also contribute to the progression of AD. Here, we sought to understand how inflammation affects the properties of the brain microvascular endothelial cells (BMECs) that compose the blood-brain barrier (BBB), which is impaired in AD. A fully human *in vitro* BBB model with brain microvascular endothelial cells derived from induced pluripotent stem cells and differentiating neural stem cell (NSC)-derived astrocytic cells was used to investigate the effects of neuroinflammation on barrier function. The cytokines TNF- $\alpha$  and IL-6 directly cause BBB dysfunction measured by a decrease in transendothelial electrical resistance, an increase in sodium fluorescein permeability, and a decrease in cell polarity, providing a link between neuroinflammation and specific aspects of BBB breakdown. A NSC-derived astrocytic cell population was added to the model and secreted cytokines and chemokines were quantified in monoculture and coculture both in the presence and absence of TNF- $\alpha$  and IL-6. Increased concentrations of pro-inflammatory cytokines known to be secreted by astrocytes or endothelial cells such as MCP-1, IL-8, IP-10, MIP-1 $\beta$ , IL-1  $\beta$ , MIG, and RANTES peaked in inflammatory conditions when NSC-astrocytic cells were present. Despite the presence of several pro-inflammatory cytokines, the NSC-derived astrocytic cells mitigated the effects of inflammation measured by a restoration of transendothelial electrical resistance and IgG permeability. These results also suggest a breakdown in transcellular transport that precedes any increase in paracellular permeability in neuroinflammation. This model has the potential to resolve questions about neurodegenerative disease progression and delivery of therapeutics to the brain.

**KEYWORDS:** human induced pluripotent stem cells, neural stem cells, astrocytes, human brain microvascular endothelial cells, tumor necrosis factor alpha, interleukin 6

## ABBREVIATIONS

A $\beta$      amyloid- $\beta$   
 AD     Alzheimer's disease  
 TNF- $\alpha$  tumor necrosis factor alpha

IL	interleukin
CSF	cerebrospinal fluid
MCI	mild cognitive impairment
BMEC	brain microvascular endothelial cell
BBB	blood-brain barrier
NVU	neurovascular unit
iPSC	induced pluripotent stem cells
TEER	transendothelial electrical
NSC	neural stem cells
NSCMM	NSC maintenance medium
DPBS	Dulbecco's Phosphate Buffered Saline
ADM	astrocyte differentiation medium
P-gp	P-glycoprotein
GFAP	glial fibrillary acidic protein
EC	endothelial cell
IFN	interferon
IVIG	intravenous immunoglobulin
BMP4	bone morphogenetic protein 4
MCP1	monocyte chemotactic protein 1
IP-10	interferon gamma-induced protein 10
MIG	monokine induced by gamma interferon
MIP-1 $\alpha$	macrophage inflammatory protein 1 alpha

## INTRODUCTION

Alzheimer's disease (AD) is a neurodegenerative disease that is the most common cause of dementia. AD pathology is characterized by extracellular amyloid- $\beta$  ( $A\beta$ ) plaques and neurofibrillary tangles in neurons which together lead to neuronal death and cognitive loss. Once believed to be a secondary response in AD, there is increasing evidence that inflammation also contributes to AD progression (reviewed by Heppner, Ransohoff, & Becher, 2015). Both systemic inflammation (e.g. from chronic disease) and central nervous system inflammation (e.g. after traumatic brain injury) can be risk factors for AD (Holmes et al., 2009; Kyrkanides et al., 2011; Mayeux et al., 1993).

Tumor necrosis factor alpha (TNF- $\alpha$ ) and interleukin (IL)-6 are two of the most commonly studied cytokines with respect to neuroinflammation in AD. A meta-analysis by Brosse et al. (2014) revealed a correlation between increased TNF- $\alpha$  and IL-6 blood or cerebrospinal fluid (CSF) in patients with severe AD compared to patients with mild cognitive impairment (MCI) or less severe AD (although several studies reviewed by Brosse et al. revealed no correlation). Additionally, brain microvessels from patients with AD have been shown to secrete increased levels of inflammatory molecules, including IL-6 and TNF- $\alpha$ , compared with age matched healthy individuals (Grammas and O'vase, 2001).

In addition to neuroinflammation, vascular pathology may also contribute to AD. Human and animal model studies suggest that dysfunction of the blood-brain barrier (BBB) plays a critical role in the progression of AD and may precede the onset of neurodegeneration and cognitive decline (Bell and Zlokovic, 2009). The blood-brain barrier comprises the brain microvascular endothelial cells (BMECs) that line cerebral capillaries and these BMECs restrict and control the movement of molecules between the blood and the brain. Together with other cells of the neurovascular unit (NVU) such as astrocytes and pericytes, BMECs tightly regulate the neuronal microenvironment for proper function (Abbott et al., 2006).

Considerable progress has been made towards modeling the NVU *in vitro*, particularly from human stem cell sources, which mitigate availability and variability issues inherent to primary cell

sources. BMECs derived from human induced pluripotent stem cells (iPSCs) exhibit an *in vivo*-like barrier phenotype, characterized by the presence of BMEC-specific proteins, functional and polarized molecular transport via proteins such as P-glycoprotein, high transendothelial electrical resistance (TEER), and low permeability to most molecules (Lippmann et al., 2014, 2012). The addition of other cell types of the NVU, such as astrocytes and pericytes (Lippmann et al., 2014), iPSC-derived astrocytes and neurons (Canfield et al., 2017), differentiating neural progenitor cells (Lim et al., 2007; Lippmann et al., 2011; Weidenfeller et al., 2007) and neural stem cells (NSCs) (Appelt-Menzel et al., 2017) improve the barrier phenotype of BMECs grown *in vitro*. Such *in vitro* BBB models can be used with different levels of complexity to elucidate contributions of different cell types and to further understanding of how different cell types can mitigate or exacerbate neurodegenerative disease.

This work aims to investigate the effects of neuroinflammation and crosstalk between cells of the NVU towards understanding the contributions of these two factors on BBB function in neurodegenerative diseases such as AD. Through the use of an *in vitro* model system with all cell components entirely derived from human stem cells, we first investigated the effects of inflammation via TNF- $\alpha$  and IL-6 on the barrier properties of iPSC-derived BMECs (Lippmann et al., 2014, 2012; Stebbins et al., 2016). Human NSC-derived astrocytic cells (Kleiderman et al., 2016) were added to the *in vitro* model and molecular crosstalk between NSC-astrocytic cells and BMECs in inflammation via secretion of cytokines and chemokines was measured. Finally, we investigated the ability of NSC-derived astrocytic cells to mitigate the effects of inflammation on the barrier function of the BBB.

## MATERIALS & METHODS

### *NSC culture & differentiation*

iPSC-derived BC1 HIP™ Neural Stem Cells (MTI-GlobalStem) were maintained on 6-well plates (Corning, Corning, NY) coated with a 1:200 solution of Corning2Geltrex™ LDEV-Free Reduced Growth Factor Basement Membrane Matrix (Thermo Fisher Scientific) in Dulbecco Modified Eagle's Medium:Nutrient Mixture F-12 (DMEM/F12) with HEPES (Thermo Fisher Scientific) and incubated at room temperature for 1 hour prior to use. NSCs were maintained in NSC Maintenance Medium (NSCMM) consisting of NeuralX NSC Medium (MTI-GlobalStem) with GS22 Neural Supplement (50X; MTI-GlobalStem), MEM Non-Essential Amino Acids (100X; Thermo Fisher Scientific), and GlutaGo (100X; Corning), supplemented with 20 ng/mL Human FGF2 Recombinant Protein (MTI-GlobalStem). Medium was changed every other day and cells were passaged every 3-4 days at 95% confluence using StemPro Accutase (Thermo Fisher Scientific) and seeded at a density of  $2 \times 10^5$  cells/cm<sup>2</sup>.

To differentiate NSCs into an astrocytic population, 24-well plates (for coculture; Corning) or 8-well chambered coverglass (for immunocytochemistry; Celvis) were pretreated with 10 µg/mL poly-L-ornithine hydrobromide (Sigma-Aldrich) at 37 °C for 1 hour, rinsed with Dulbecco's Phosphate Buffered Saline (DPBS; Thermo Fisher Scientific), and incubated with 1% laminin (Sigma-Aldrich) at 37 °C for 1 hour. NSCs were dissociated using StemPro Accutase and seeded on pretreated plates or coverglass chambers at a density of  $5 \times 10^5$  cells/cm<sup>2</sup>. Medium was switched to astrocyte differentiation medium (ADM), consisting of NSCMM supplemented with 20 ng/mL bone morphogenetic protein 4 (BMP4; R&D Systems). Media changes occurred every other day until coculture with BMECs was initiated after 5-10 days.

### *iPSC-BMEC differentiation and model set up*

iPS(IMR90)-4 iPSCs (WiCell) (Yu et al., 2007) were maintained and differentiated as previously described (Lippmann et al., 2014; Mantle et al., 2016). Briefly, iPSCs were maintained in mTeSR1

medium (STEMCELL Technologies) on 6-well plates coated with 83.3 µg/mL growth factor-reduced Matrigel (Thermo Fisher Scientific) in DMEM/F-12. Cells were passaged every 3-5 days using Versene (Thermo Fisher Scientific) and mechanical dissociation. Cells were differentiated as described by (Lippmann et al., 2014; Mantle et al., 2016). Differentiated BMECs (Day 9) were passaged to 24-well Transwell cell culture inserts (PET; 0.4 µm pores; Fisher Scientific) pretreated for a minimum of four hours with 40% collagen IV (Sigma-Aldrich) and 10% fibronectin (Sigma-Aldrich). The Transwell inserts were placed into 24-well plates or 24-well plates containing differentiated astrocytic cells for coculture, and all medium was switched to endothelial cell medium consisting of human endothelial cell serum free medium (Thermo Fisher Scientific) supplemented with 1% platelet-poor derived serum (EC-media). Experiments were performed after 48 hours of coculture unless otherwise noted.

To mimic neuroinflammation, cells were incubated with 10 ng/mL of recombinant human TNF- $\alpha$  (R&D Systems), 10 ng/mL IL-6 (R&D Systems), or 10 ng/mL each of both cytokines (inflammatory media). Cytokines were added to the media in both the luminal and abluminal compartments after BMECs were incubated for 24 hours on inserts.

#### ***NSC-derived astrocytic population immunocytochemistry and confocal microscopy***

All solutions were prepared in DPBS. NSCs at different stages of differentiation on 8-well chambered coverglass were washed once with DPBS and fixed using 2% paraformaldehyde (Electron Microscopy Sciences) for 15 minutes. Following three DPBS washes, the cells were permeabilized with 0.1% Triton X-100 (Sigma-Aldrich) for 5 minutes and blocked in 10% goat serum (Sigma-Aldrich) for 1 hour. Cells were incubated with primary antibody solution (mouse anti-glial fibrillary acidic protein (GFAP) and mouse anti-nestin purchased from Thermo Fisher Scientific; mouse anti-nestin purchased from Abcam; Table 1) overnight at 4 °C on an orbital shaker. The cells were rinsed twice with 1% goat serum and incubated with secondary antibody solution at room temperature for 1 hour on an orbital shaker. Cells were rinsed twice with 1% goat serum and stored in DPBS at 4 °C until imaging. Fifteen minutes prior to imaging, one drop of NucBlue Fixed Cell ReadyProbes Reagent (ThermoFisher



Scientific) was added to each chamber. Images were taken with a 20x objective on a Zeiss LSM 710 confocal microscope (Zeiss).

1° Antibody	Dilution	2° Antibody	Conc (µg/mL)
Mouse anti-Nestin	1:500	Goat anti-mouse AlexaFluor 568	5
Chicken anti-Vimentin	1:5000	Goat anti-chicken AlexaFluor 488	5
Rabbit anti-GFAP	1:1000	Goat anti-rabbit AlexaFluor 647	1

**Table 1:** Antibodies used in immunocytochemistry of NSC-derived astrocytic cells

### ***Transendothelial electrical resistance (TEER) measurements***

Cell culture inserts containing BMECs were transferred to an Endohm-6 chamber (World Precision Instruments) containing EC- media. An EVOM2 Epithelial Volt Meter (World Precision Instruments) was used to measure the resistance of the cell monolayer and membrane. To calculate the TEER value, the measured resistance of a blank treated Transwell insert was subtracted from each experimental measured value and then multiplied by the membrane surface area.

### ***Sodium fluorescein permeability assay***

Media in the bottom compartment was aspirated and replaced with 600 µL transport buffer, consisting of 10 mM HEPES, 0.1% (w/v) bovine serum albumin and 4.5% (w/v) glucose (Sigma-Aldrich). Media in the top compartment was aspirated and replaced with 100 µL of 100 µM sodium fluorescein (Sigma-Aldrich) in transport buffer. Samples were collected every 15 minutes for 1 hour by removing 100 µL from the bottom compartment and transferring it to a 96-well plate. 100 µL transport buffer was replaced in the bottom compartment to maintain constant volume. A Spectra Max M5 microplate reader (Molecular Devices) was used to analyze the 96-well plate for fluorescence (excitation = 460 nm, emission = 515 nm). The solute permeability coefficient  $P_s$  was calculated using the equation,

$$P_s = \frac{C_A * V_A}{t * S * C_L}$$

where  $C_A$  and  $C_L$  are the abluminal and luminal concentrations respectively,  $V_A$  is the abluminal volume,  $t$  is the time and  $S$  is the surface area of the membrane. The inverse of the permeability of a blank treated insert was subtracted from the inverse of  $P_s$  to obtain the permeability of the cell monolayer. Dilution due to sample removal and addition of transport buffer to maintain volume was accounted for in the calculation (Deli et al., 2005).

### ***P-glycoprotein efflux assay***

The transport rate of the fluorescent P-glycoprotein (P-gp) substrate Rhodamine 123 (Sigma-Aldrich) was measured in the luminal to abluminal and abluminal to luminal directions. All medium was aspirated from both compartments and replaced with EC-media in the receiving compartments and EC-media containing 10  $\mu$ M Rhodamine 123 in the donor compartments. Samples of 100  $\mu$ L were collected in a 96-well plate every hour for three hours. Medium was replaced to maintain constant volume and dilutions were accounted for in the calculations. The amount of Rhodamine 123 transported per unit time was calculated as the transport rate in each direction. The efflux ratio was calculated by dividing the rate in the abluminal to luminal direction by the rate in the luminal to abluminal direction.

### ***IgG quantification assay***

BMECs were grown in monoculture or coculture, cytokines or control media were added on Day 1 of coculture. On Day 2, 10 mg/mL Gammagard Liquid Immune Globulin Intravenous (Human) 10% (IVIG; Lot # LE12L017AB; Baxter) was added to the luminal compartment and cells were incubated at 37 °C for 6 hours. Abluminal samples were collected and stored at -20 °C until quantification. The Easy-Titer ® Human IgG Assay Kit (Thermo Fisher Scientific) was used according to the manufacturer's protocol to quantify the amount of IgG in the abluminal compartment after 6 hours.

### ***Cytokine quantification by Luminex***

BMECs were grown in monoculture or coculture, 10 ng/mL each of TNF- $\alpha$  and IL-6 were added to appropriate wells on Day 1. On Day 2 media from the abluminal compartments were collected and stored at -20 °C until analysis. The Cytokine 25-Plex Human Panel (Thermo Fisher Scientific) assay and Luminex 100/200 system (Thermo Fisher Scientific) were used according to the manufacturer's instructions to quantify cytokines and chemokines in the abluminal samples. Samples were diluted 1:2 per the instructions. All measurements below the limit of detection were treated as a concentration of 0 pg/mL for statistical analysis.

### ***Experimental Design and Statistical Analyses***

JMP<sup>®</sup> v13.0 (SAS Institute Inc.) was used for statistical analysis. Statistical evaluation of data was performed using Student's t-test and analysis of variance (ANOVA) with  $\alpha = 0.05$ . To determine statistical significance of the effects of coculture and TNF- $\alpha$ /IL-6 media on TEER, IgG transport and Luminex assay results, a least squares fit was performed. Error bars in figures represent standard error of the mean calculated over three independent experiments unless otherwise noted.

## **RESULTS**

### ***TNF- $\alpha$ and IL-6 treatment impairs barrier integrity***

To investigate the effects of inflammation directly on the endothelial cells of the BBB, iPSC-derived BMECs were incubated with IL-6, TNF- $\alpha$  or both cytokines for 24 hours. TEER, a measure of barrier integrity, was unchanged after the addition of IL-6 alone but was reduced by 13% and 16% after the addition of TNF- $\alpha$  and both cytokines respectively (Figure 1A; unpaired t-test;  $p = 0.033$  and  $p = 0.007$ ). Permeability to sodium fluorescein, a measure of paracellular permeability, was 2- to 2.5-fold higher than the control with the addition of inflammatory cytokines (Figure 1B; unpaired t-test;  $p = 0.005$ ,  $p = 0.021$  and  $p = 0.048$ ). Transport of the fluorescent P-gp substrate Rhodamine 123 was measured in both the luminal to abluminal and abluminal to luminal directions (Figure 1C). The efflux ratio, or the

ratio of the amount transported out of the brain compartment to the amount transported into the brain compartment, decreased in the presence of inflammatory cytokines. The efflux ratio in the cells in the inflammation cases was about 40% lower than the control case and is evidence for a loss in polarity in BMECs. Together, these results suggest that the cytokines TNF- $\alpha$  and IL-6 can directly impair BBB integrity.

**Figure 1: Barrier integrity with inflammation.** Barrier integrity of iPSC-BMECs after incubation with the cytokines TNF- $\alpha$  and IL-6 measured by (A) TEER (B) sodium fluorescein permeability (normalized to the control) and (C) efflux ratio (abluminal to luminal transport rate/luminal to abluminal transport rate) of the P-gp substrate Rhodamine 123. (n=4; two biological replicates and two independent experiments; data represents the mean  $\pm$  standard error of the mean; \* p<0.05; \*\* p < 0.01)

#### ***Coculture with NSC-derived astrocytic cells improves TEER***

Crosstalk between BMECs and other cell types of the NVU *in vivo* is important for maintaining a properly functioning BBB therefore to investigate this crosstalk between cell types, astrocytic cells were differentiated from NSCs. Immunocytochemistry was used to characterize the cells both before and after differentiation. NSCs expressed nestin, an NSC marker, and vimentin, often used as an astrocyte marker, but lacked GFAP expression, a mature astrocyte marker (Figure 2A, top). After five days of differentiation, the cells still showed expression of nestin and had increased intensity of vimentin (Figure 2A, bottom). Subpopulations of cells also expressed GFAP (Figure 2A, bottom) and  $\beta$ III tubulin (SI Figure 2). Cell morphology changed by day 5 from NSC to the more astrocyte characteristic phenotype with a star shape and endfoot processes.

After 5-10 days of differentiation, NSC-derived astrocytic cells were cocultured with iPSC-derived BMECs for a fully human coculture model of the BBB. With the addition of NSC-astrocytic cells, BMECs had a 15% increase in TEER over the monoculture case (Figure 2B). This effect was consistent for NSCs differentiated for five or ten days (data not shown) and therefore a differentiation time of five days was used for all subsequent experiments.

**Figure 2: NSC-astrocytic cell population characterization.** (A) NSCs (top) and cells that have been differentiated for five days (bottom) immunostained for nestin (red), vimentin (green), and GFAP (magenta). Nuclei stained with DAPI (blue). Scale bars 100  $\mu$ m. (B) Representative Day 2 TEER of BMECs cocultured with 5 day differentiated (+5D) NSC-astrocytic cells and monoculture without astrocytic cells (n = 3; representative figure; data represents the mean  $\pm$  standard error of the mean; p = 0.0004). (C) iPSC differentiation into BMECs was initiated first, followed by NSC differentiation into astrocytic cells in parallel. On Day 0, coculture was initiated by passaging the differentiated BMECs onto transwell inserts and placing them into 24-well plates containing the differentiated NSCs. Cytokines were added one day after coculture initiation and experiments were carried out 24 and 48 hours later.

### ***Cytokine and chemokine crosstalk between BMECs and NSC-derived astrocytic cells***

BMECs were grown in monoculture or coculture with NSC-derived astrocytic cells, and 10 ng/mL each of TNF- $\alpha$  and IL-6 were added in the inflammation cases. After 24 hours, abluminal media was collected and 25 cytokines and chemokines were quantified using a Luminex multiplexed assay (Figure 2C). Of the 25 analytes, 17 were quantified in at least one culture condition. Two were present in all cases (monocyte chemoattractant protein 1; MCP-1; interferon gamma-induced protein 10; IP-10), two were present only when NSC-astrocytic cells were present (IL-8 and interferon alpha; IFN- $\alpha$ ), eight were measured in the inflammation cases only (IL-2R, IL-4, IL-7, IL-12, monokine induced by gamma interferon; MIG; macrophage inflammatory protein 1 alpha; MIP-1 $\alpha$ ; IL-6, and TNF- $\alpha$ ) and four were detected in the inflammation coculture case only (IFN- $\gamma$ , IL-1 $\beta$ , MIP-1 $\beta$ , RANTES). Nine analytes were below the limit of quantitation (Eotaxin, IL-1RA, IL-2, IL-5, IL-10, IL-13, IL-15 and IL-17).

An NSC-derived astrocytic population-only case was also analyzed in control and inflammation conditions (SI Figure 1). Only MCP-1 was detected in both cases while eight other cytokines were detected in the NSC-derived astrocytic inflammation case. Two cytokines (IL-10, IL-5) were detected in the presence of the NSC-derived astrocytic population but were not detected in any cases with BMECs present. Five cytokines (MCP-1, IP-10, IL-22, IFN- $\alpha$ , IL-8) were measured in the NSC-derived astrocytic

inflammation media but were present at significantly higher concentrations in the coculture inflammation case. Lastly, two cytokines (IL-7 and IL-4) were measured at about two orders of magnitude higher concentrations in the NSC-derived astrocytic inflammation case than the coculture inflammation case.

MCP-1, a chemokine commonly associated with inflammation in neurodegenerative disease and injury, was measured in all cases (Figure 3A). There was a 24- and 33-fold increase of MCP-1 from monoculture to coculture in the control and inflammation cases respectively. Additionally, there was a 6- and 8-fold increase in MCP-1 concentration from the control to inflammatory conditions in monoculture and coculture cases respectively. Here, MCP-1 is secreted by BMECs (and potentially astrocytic cells as well) and both coculture and inflammation elevate MCP-1 levels, although coculture has a greater effect. A second chemokine, interferon gamma-induced protein 10 (IP-10) was measured in all cases (Figure 3B). There was an approximately 50-fold increase in IP-10 levels in the coculture with TNF- $\alpha$  and IL-6 case over the controls.

The two cytokines, IL-8 and IFN- $\alpha$ , were measured only in the inflammatory conditions, in both monoculture and coculture (Figure 3C). With the presence of NSC-derived astrocytic cells, IL-8 concentration increased 71-fold over the monoculture conditions. There was a 10-fold increase in IFN- $\alpha$  concentration between the monoculture and coculture cases as well. These two cytokines are secreted by BMECs in response to TNF- $\alpha$  and IL-6 and we hypothesize their expression is exacerbated in response to other soluble factors present in coculture.

The largest group of cytokines was measured in the coculture cases only, both in the control and inflammatory conditions (Figure 3D). The highest levels of cytokines were measured in the inflammation cases, with increases ranging from 1.2 to 4-fold for MIP-1 $\alpha$  and MIG over the control. This group of cytokines is likely able to be secreted by the NSC-derived astrocytic population, or is secreted by endothelial cells in response to a factor only present when NSC-astrocytic cells are present.

A group of five cytokines were only detected with inflammation in coculture (Figure 3E). This group included IFN- $\gamma$ , IL-1 $\beta$ , MIP-1 $\beta$ , and RANTES. Of these cytokines, IFN- $\gamma$  and IL-1 $\beta$  concentrations

were low and very close to the LOQ while MIP-1 $\beta$  and RANTES were detected at higher levels of 22 and 296 pg/mL respectively.

**Figure 3: Concentrations of cytokines and chemokines measured by Luminex assay.** Abluminal concentrations of 25 human cytokine and chemokines were measured after 24 hours of incubation with TNF- $\alpha$  and IL-6 or control media for cells grown in monoculture or coculture. Of the 25 cytokines assayed, 17 were measured in at least one case above the limit of quantitation. (A) MCP-1 and (B) IP-10 were measured in all four cases tested. (C) IFN- $\alpha$  and IL-8 were measured in the inflammatory cases for both monoculture and coculture. (D) Six cytokines were measured only in coculture cases with both control and inflammation media. (E) Four cytokines were measured only in the coculture wells with TNF- $\alpha$  and IL-6 media and were below the limit of quantitation in the other three cases.

***NSC-derived astrocytic cells mitigate barrier dysfunction associated with TNF- $\alpha$  and IL-6 inflammation***

TEER of BMECs in monoculture or coculture with NSC-derived astrocytic cells was measured 24 and 48 hours after the addition of cytokine or control media to assess barrier integrity (Figure 4). For BMECs in monoculture, there was a 21% difference at 24 hours between the control and inflammatory conditions. In contrast, in coculture over the same timeframe, the TEER in inflammatory conditions was 12% lower than the control. This difference between monoculture and coculture is more significant 48 hours after the addition of TNF- $\alpha$  and IL-6 where the difference between TEER in control and inflammatory case was 56% for monoculture, but remained similar at 13% in coculture.

TEER values for monoculture cells dropped 17% and 54% between Day 2 and Day 3 for control and inflammatory conditions respectively, revealing that the addition of cytokines induces a barrier breakdown that is exacerbated with time in this model. In contrast, TEER values for coculture cells dropped 7.1% for the control and 8.5% for inflammatory conditions, suggesting that NSC-derived astrocytic cells help maintain BBB function during inflammation.

**Figure 4: TEER of BMECs grown in monoculture or coculture with NSC-derived astrocytic cells with TNF- $\alpha$  and IL-6.** iPSC-derived BMECs were grown in monoculture or coculture with NSC-derived astrocytic cells and

TEER was measured 24 (gray) and 48 (black) hours after the addition of TNF- $\alpha$  and IL-6 or control media. (n=6; three biological replicates and two independent experiments; mean  $\pm$  standard error of the mean)

IgG transport across the BBB was quantified as a second measure of barrier integrity. IgG extravasation is often used as an *in vivo* measure of barrier integrity after disease or injury. After 24 hours of incubation with cytokine or control media, 10 mg/mL IgGs were added to the luminal compartment to mimic plasma levels and quantified in the abluminal compartment 24 hours later. The amount of IgG transported from the luminal to abluminal compartment was affected by both inflammation and culture conditions (Figure 5; least squares fit;  $p = 0.0204$  &  $p = 0.0305$  respectively). The amount of IgG transported in monoculture with inflammation was about 2.8-fold higher than the monoculture control (unpaired t-test;  $p = 0.0489$ ). However both the control and TNF- $\alpha$ /IL-6 cases in coculture were not statistically different than the monoculture control. With BMECs alone, there is an increase in IgG transport in inflammation and this increase is mitigated by the presence of NSC-derived astrocytic cells.

**Figure 5: Luminal to abluminal IgG transport in coculture with TNF- $\alpha$  and IL-6.** iPSC-derived BMECs were grown in monoculture or coculture with NSC-derived astrocytic cells and incubated with cytokine media or control media for 24 hours before 10mg/mL IVIG was added to the luminal compartment. Abluminal IgG concentration was measured at 24 hours. (n=6; three biological replicates and two independent experiments; mean  $\pm$  standard error of the mean; \*  $p < 0.05$ )

## DISCUSSION

*In vitro* BBB models facilitate the study of transport phenomena at the cellular level and allow for different levels of complexity through the incorporation of different cell types. To investigate the effects of astrocytes on BMECs during inflammation, we used a fully human BBB model with cells derived entirely from stem cell sources. iPSCs were differentiated into BMECs while in parallel NSCs were differentiated into an astrocytic population and these were combined in a non-contact coculture. The NSC-derived cells expressed two astrocytic markers vimentin and GFAP, however these cells still expressed the NSC marker nestin and a subpopulation also expressed the neuronal marker  $\beta$ III tubulin. Kleiderman et al., (2016) have shown that both NSCs and astrocytes derived from mouse embryonic stem



cells express nestin, although a decrease in expression levels is indicative of a differentiated state. Despite a heterogeneous population of cells, these NSC-astrocytic cells still had a profound effect on the barrier properties of the BMECs as measured by an improvement in TEER.

Before investigating the effects of NSC-derived astrocytic cells on the BBB in inflammation, a baseline response was first established using BMECs alone. Although the reduction in TEER was significant in the presence of TNF- $\alpha$ , TEER values of 3000  $\Omega \cdot \text{cm}^2$  are high and are still within an expected *in vivo* range of 1500-6000  $\Omega \cdot \text{cm}^2$  (Butt et al., 1990). Additionally, these values around 3000  $\Omega \cdot \text{cm}^2$  exceed the minimum TEER transport threshold of 500  $\Omega \cdot \text{cm}^2$ , above which paracellular permeability of small molecules, such as sodium fluorescein, does not change (Mantle et al., 2016). It is unlikely that there is any change to organization of tight junction structure at this high TEER value. Therefore, it is unexpected to see a significant 2- to 2.5-fold increase in sodium fluorescein permeability in the presence of IL-6 and TNF- $\alpha$ . These results, coupled with a decrease in polarity as measured by a decreased P-gp efflux ratio (which may be caused by a number of mechanisms including loss of P-gp polarity, decreased expression of P-gp, and inactivation of P-gp), are consistent with transcellular transport increases in inflammation prior to a significant breakdown of paracellular permeability. An increase in vesicular transcytosis without a breakdown in paracellular permeability has been shown in other pathological conditions such as hypoxia, ischemia, and injury (De Bock et al., 2016). Furthermore, our lab has demonstrated increases in uptake of endocytic pathway probes in the iPSC-BMEC model in disease states (Mantle and Lee, unpublished). Additionally, it is clear that TNF- $\alpha$  and IL-6 act directly on the cells of the BBB and can cause barrier dysfunction. Further characterization of BMEC response to inflammation by examining upregulation of cell adhesion molecules and selectins could provide a better understanding of precisely how these inflammatory cues affect BBB integrity.

Another potential contribution to barrier dysfunction in disease is additional pro-inflammatory molecules that are secreted by astrocytes or BMECs in response to inflammation. During insults such as infection, inflammation, trauma, and neurodegeneration, astrocytes can enter a reactive state that results in local pro-inflammatory conditions (Broux et al., 2015). In the presence of inflammatory media in

coculture, there was a significant increase in the number and concentration of several cytokines and chemokines that are well-known for their pro-inflammatory properties.

For every cytokine detected, the highest levels were measured in the coculture inflammation case when crosstalk between the two cell types was possible. Astrocytes are known to secrete pro-inflammatory MCP-1, IP-10, MIP-1 $\beta$ , IL-1  $\beta$ , MIG, and RANTES, as well as IL-15, IL-17 and anti-inflammatory IL-10, which were below LOQ (Sofroniew, 2015; Wang et al., 2014; Williams et al., 2009; Xia et al., 2000). BMECs can also be a source of pro-inflammatory chemokines including MCP-1, IL-8, IP-10 and RANTES, which are important for immune cell recruitment to the brain (reviewed by Ransohoff, Schafer, Vincent, Blachère, & Bar-Or, 2015). MCP-1 is a chemokine responsible for recruitment of leukocytes to the brain, it can compromise BBB integrity through reorganization of tight junction proteins, and increased levels of MCP-1 are associated with neurodegeneration and neuroinflammation (Yao and Tsirka, 2014). Additionally, MCP-1 has been shown to be upregulated in the CSF of patients with MCI and AD (Brosseron et al., 2014). IP-10 is also responsible for immune cell recruitment to the brain and can be secreted by both astrocytes and endothelial cells (Shimizu et al., 2015). MIP-1 $\beta$  is known to be expressed by a subpopulation of astrocytes in AD in coordination with IP-10 (Xia et al., 2000). IL-1 $\beta$  is known to increase BBB permeability via the downregulation of SHH in astrocytes (Wang 2014). MIG has been shown to be elevated in the plasma of AD patients compared to patients with MCI and healthy controls (Lee et al., 2008). Finally, several cytokines detected in this study including IL-1 $\beta$ , MCP-1 and IL-8 (as well as IL-6 and TNF- $\alpha$ ) have been shown to be present in higher levels in microvessels from patients with AD compared to age matched controls (Grammas and O'vase, 2002, 2001). The results from these studies are consistent with known key molecules in inflammation associated with neurodegenerative disease.

There were several cytokines and chemokines detected that are not commonly associated with astrocytes or endothelial cells in AD or neuroinflammation, namely IFN- $\alpha$ , IL-2R, and IL-7. Other cytokines identified are more commonly associated with microglia, including MIP-1 $\alpha$ , IL-4, and IL-12. MIP-1 $\alpha$  was detected in both coculture conditions however it is known to be expressed by microglia *in*

*vitro* in response to aggregated A $\beta_{1-42}$  (Lue et al., 2001). Levels of the anti-inflammatory IL-4 were slightly elevated in inflammation coculture compared to the control and were not detected in either monoculture case. Overexpression of IL-4 in the hippocampus of a mouse model of AD resulted in increased deposition of A $\beta$ , while an earlier study showed that CNS overexpression of IL-4 attenuated AD progression in a mouse model (Kiyota et al., 2010) so the role of this cytokine in disease is still unclear. IL-12 is part of the inflammatory response to A $\beta$  and associated with a pro-inflammatory microglial state (Heppner et al., 2015). This *in vitro* coculture model could potentially be used to identify new molecular mechanisms in inflammation and neurodegenerative disease.

Despite the presence of many pro-inflammatory cytokines and chemokines and only one potentially anti-inflammatory cytokine, NSC-astrocytic cells mitigated the barrier dysfunction associated with TNF- $\alpha$  and IL-6 incubation. While TEER values in inflammation were lower in both monoculture and coculture when compared to the controls, the presence of NSC-astrocytic cells mitigated the effects of inflammation over time and helped to maintain barrier integrity. TEER in all cases remained above the 1000  $\Omega \cdot \text{cm}^2$  large molecule transport threshold, above which the permeability of large molecules, including IgGs, does not change (Mantle et al., 2016). However in monoculture with TNF- $\alpha$  and IL-6, there is a significant increase in IgG transport across the BBB, which is not present in the coculture case. Although there is conflicting literature about the exact mechanism of IgG transport at the BBB (Deane et al., 2005; Garg and Balthasar, 2009; Schlachetzki et al., 2002; Yip et al., 2014), these data further support the hypothesis that transcellular permeability is compromised before paracellular permeability in inflammatory conditions.

## CONCLUSIONS

These results demonstrate that the cytokines TNF- $\alpha$  and IL-6 act directly on the BMECs of the BBB and a transcellular breakdown occurs before paracellular permeability is impaired. This effect is mitigated by the presence of an NSC-derived astrocytic population, even though there is a significant

increase in several pro-inflammatory cytokines known to impair BBB function. This model mimics cellular responses to inflammation at the BBB and can provide a way to study the contributions of individual cell types to disease progression. These results highlight the complex nature of inflammation in neurodegenerative disease and suggest a delicate balance of soluble factors that impact the function of the BBB.

## REFERENCES

- Abbott, N.J., Rönnebeck, L., Hansson, E., 2006. Astrocyte-endothelial interactions at the blood-brain barrier. *Nat. Rev. Neurosci.* 7, 41–53. <https://doi.org/10.1038/nrn1824>
- Appelt-Menzel, A., Cubukova, A., Günther, K., Edenhofer, F., Piontek, J., Krause, G., Stüber, T., Walles, H., Neuhaus, W., Metzger, M., 2017. Establishment of a Human Blood-Brain Barrier Co-culture Model Mimicking the Neurovascular Unit Using Induced Pluri- and Multipotent Stem Cells. *Stem Cell Reports* 8, 894–906. <https://doi.org/10.1016/j.stemcr.2017.02.021>
- Bell, R.D., Zlokovic, B. V., 2009. Neurovascular mechanisms and blood-brain barrier disorder in Alzheimer's disease. *Acta Neuropathol.* 118, 103–113. <https://doi.org/10.1007/s00401-009-0522-3>
- Brosseron, F., Krauthausen, M., Kummer, M., Heneka, M.T., 2014. Body Fluid Cytokine Levels in Mild Cognitive Impairment and Alzheimer's Disease: A Comparative Overview. *Mol. Neurobiol.* 50, 534–544. <https://doi.org/10.1007/s12035-014-8657-1>
- Broux, B., Gowing, E., Prat, A., 2015. Glial regulation of the blood-brain barrier in health and disease. *Semin. Immunopathol.* 37, 577–590. <https://doi.org/10.1007/s00281-015-0516-2>
- Butt, A.M., Jones, H.C., Abbott, N.J., 1990. Electrical resistance across the blood-brain barrier in anaesthetized rats: a developmental study. *J. Physiol.* 429, 47–62. <https://doi.org/10.1113/jphysiol.1990.sp018243>
- Canfield, S.G., Stebbins, M.J., Morales, B.S., Asai, S.W., Vatine, G.D., Svendsen, C.N., Palecek, S.P., Shusta, E. V., 2017. An isogenic blood-brain barrier model comprising brain endothelial cells, astrocytes, and neurons derived from human induced pluripotent stem cells. *J. Neurochem.* 140, 874–888. <https://doi.org/10.1111/jnc.13923>
- De Bock, M., Van Haver, V., Vandenbroucke, R.E., Decrock, E., Wang, N., Leybaert, L., 2016. Into rather unexplored terrain—transcellular transport across the blood-brain barrier. *Glia* 64, 1097–1123. <https://doi.org/10.1002/glia.22960>
- Deane, R., Sagare, A., Hamm, K., Parisi, M., LaRue, B., Guo, H., Wu, Z., Holtzman, D.M., Zlokovic, B. V., 2005. IgG-assisted age-dependent clearance of Alzheimer's amyloid beta peptide by the blood-brain barrier neonatal Fc receptor 1. *J. Neurosci.* 25, 11495–11503.
- Deli, M. a., Ábrahám, C.S., Kataoka, Y., Niwa, M., 2005. Permeability studies on in vitro blood-brain barrier models: Physiology, pathology, and pharmacology. *Cell. Mol. Neurobiol.* 25, 59–127. <https://doi.org/10.1007/s10571-004-1377-8>
- Garg, A., Balthasar, J.P., 2009. Investigation of the Influence of FcRn on the Distribution of IgG to the Brain. *AAPS J.* 11, 553–557. <https://doi.org/10.1208/s12248-009-9129-9>
- Grammas, P., O'vase, R., 2002. Cerebrovascular transforming growth factor- $\beta$  contributes to inflammation in the Alzheimer's disease brain. *Am. J. Pathol.* 160, 1583–1587. [https://doi.org/10.1016/S0002-9440\(10\)61105-4](https://doi.org/10.1016/S0002-9440(10)61105-4)
- Grammas, P., O'vase, R., 2001. Inflammatory factors are elevated in brain microvessels in Alzheimer's disease. *Neurobiol. Aging* 22, 837–842. [https://doi.org/10.1016/S0197-4580\(01\)00276-7](https://doi.org/10.1016/S0197-4580(01)00276-7)
- Heppner, F.L., Ransohoff, R.M., Becher, B., 2015. Immune attack: the role of inflammation in Alzheimer disease. *Nat. Rev. Neurosci.* 16, 358–372. <https://doi.org/10.1038/nrn3880>

- Holmes, C., Cunningham, C., Zotova, E., Woolford, J., Dean, C., Kerr, S., Culliford, D., Perry, V.H., 2009. Systemic inflammation and disease progression in Alzheimer disease. *Neurology* 73, 768–74. <https://doi.org/10.1212/WNL.0b013e3181b6bb95>
- Kiyota, T., Okuyama, S., Swan, R.J., Jacobsen, M.T., Gendelman, H.E., Ikezu, T., 2010. CNS expression of anti-inflammatory cytokine interleukin-4 attenuates Alzheimer's disease-like pathogenesis in APP+PS1 bigenic mice. *FASEB J.* 24, 3093–3102. <https://doi.org/10.1096/fj.10-155317>
- Kleiderman, S., Sá, J. V., Teixeira, A.P., Brito, C., Gutbier, S., Evje, L.G., Hadera, M.G., Glaab, E., Henry, M., Sachinidis, A., Alves, P.M., Sonnewald, U., Leist, M., 2016. Functional and phenotypic differences of pure populations of stem cell-derived astrocytes and neuronal precursor cells. *Glia* 64, 695–715. <https://doi.org/10.1002/glia.22954>
- Kyrkanides, S., Tallents, R.H., Miller, J.H., Olschowka, M.E., Johnson, R., Yang, M., Olschowka, J.A., Brouxhon, S.M., O'Banion, M.K., 2011. Osteoarthritis accelerates and exacerbates Alzheimer's disease pathology in mice. *J. Neuroinflammation* 8, 112. <https://doi.org/10.1186/1742-2094-8-112>
- Lee, K.S., Chung, J.H., Lee, K.H., Shin, M.-J., Oh, B.H., Hong, C.H., 2008. Bioplex analysis of plasma cytokines in Alzheimer's disease and mild cognitive impairment. *Immunol. Lett.* 121, 105–109. <https://doi.org/10.1016/j.imlet.2008.09.004>
- Lim, J.C., Wolpaw, A.J., Caldwell, M.A., Hladky, S.B., Barrand, M.A., 2007. Neural precursor cell influences on blood-brain barrier characteristics in rat brain endothelial cells. *Brain Res.* 1159, 67–76. <https://doi.org/10.1016/j.brainres.2007.05.032>
- Lippmann, E.S., Al-Ahmad, A., Azarin, S.M., Palecek, S.P., Shusta, E. V, 2014. A retinoic acid-enhanced, multicellular human blood-brain barrier model derived from stem cell sources. *Sci. Rep.* 4, 4160. <https://doi.org/10.1038/srep04160>
- Lippmann, E.S., Azarin, S.M., Kay, J.E., Nessler, R.A., Wilson, H.K., Al-Ahmad, A., Palecek, S.P., Shusta, E. V, 2012. Derivation of blood-brain barrier endothelial cells from human pluripotent stem cells. *Nat. Biotechnol.* 30, 783–791. <https://doi.org/10.1038/nbt.2247>
- Lippmann, E.S., Weidenfeller, C., Svendsen, C.N., Shusta, E. V., 2011. Blood-brain barrier modeling with co-cultured neural progenitor cell-derived astrocytes and neurons. *J. Neurochem.* 119, 507–520. <https://doi.org/10.1111/j.1471-4159.2011.07434.x>
- Lue, L.F., Rydel, R., Brigham, E.F., Yang, L.B., Hampel, H., Murphy, G.M., Brachova, L., Yan, S. Du, Walker, D.G., Shen, Y., Rogers, J., 2001. Inflammatory repertoire of Alzheimer's disease and nondemented elderly microglia in vitro. *Glia* 35, 72–79. <https://doi.org/10.1002/glia.1072>
- Mantle, J.L., Min, L., Lee, K.H., 2016. Minimum Transendothelial Electrical Resistance Thresholds for the Study of Small and Large Molecule Drug Transport in a Human in Vitro Blood-Brain Barrier Model. *Mol. Pharm.* 13, 4191–4198. <https://doi.org/10.1021/acs.molpharmaceut.6b00818>
- Mayeux, R., Ottman, R., Tang, M.X., Noboa-Bauza, L., Marder, K., Gurland, B., Stern, Y., 1993. Genetic susceptibility and head injury as risk factors for Alzheimer's disease among community-dwelling elderly persons and their first-degree relatives. *Ann Neurol* 33, 494–501. <https://doi.org/10.1002/ana.410330513>
- Ransohoff, R.M., Schafer, D., Vincent, A., Blachère, N.E., Bar-Or, A., 2015. Neuroinflammation: Ways in Which the Immune System Affects the Brain. *Neurotherapeutics* 12, 896–909. <https://doi.org/10.1007/s13311-015-0385-3>

- Schlachetzki, F., Zhu, C., Pardridge, W.M., 2002. Expression of the neonatal Fc receptor (FcRn) at the blood-brain barrier. *J. Neurochem.* 81, 203–206. <https://doi.org/10.1046/j.1471-4159.2002.00840.x>
- Shimizu, F., Nishihara, H., Sano, Y., Takeshita, Y., Takahashi, S., Maeda, T., Takahashi, T., Abe, M., Koga, M., Kanda, T., 2015. Markedly increased IP-10 production by blood-brain barrier in neuromyelitis optica. *PLoS One* 10. <https://doi.org/10.1371/journal.pone.0122000>
- Sofroniew, M. V., 2015. Astrocyte barriers to neurotoxic inflammation. *Nat. Rev. Neurosci.* 16, 249–263. <https://doi.org/10.1038/nrn3898>
- Stebbins, M.J., Wilson, H.K., Canfield, S.G., Qian, T., Palecek, S.P., Shusta, E. V., 2016. Differentiation and characterization of human pluripotent stem cell-derived brain microvascular endothelial cells. *Methods* 101, 93–102. <https://doi.org/10.1016/j.jymeth.2015.10.016>
- Wang, Y., Jin, S., Sonobe, Y., Cheng, Y., Horiuchi, H., Parajuli, B., Kawanokuchi, J., Mizuno, T., Takeuchi, H., Suzumura, A., 2014. Interleukin-1 $\beta$  induces blood-brain barrier disruption by downregulating sonic hedgehog in astrocytes. *PLoS One* 9, e110024. <https://doi.org/10.1371/journal.pone.0110024>
- Weidenfeller, C., Svendsen, C.N., Shusta, E. V., 2007. Differentiating embryonic neural progenitor cells induce blood-brain barrier properties. *J. Neurochem.* 101, 555–565. <https://doi.org/10.1111/j.1471-4159.2006.04394.x>
- Williams, R., Yao, H., Dhillon, N.K., Buch, S.J., 2009. HIV-1 Tat co-operates with IFN-gamma and TNF-alpha to increase CXCL10 in human astrocytes. *PLoS One* 4, e5709. <https://doi.org/10.1371/journal.pone.0005709>
- Xia, M.Q., Bacskaï, B.J., Knowles, R.B., Qin, S.X., Hyman, B.T., 2000. Expression of the chemokine receptor CXCR3 on neurons and the elevated expression of its ligand IP-10 in reactive astrocytes: in vitro ERK1/2 activation and role in Alzheimer's disease. *J. Neuroimmunol.* 108, 227–235.
- Yao, Y., Tsirka, S.E., 2014. Monocyte chemoattractant protein-1 and the blood-brain barrier. *Cell. Mol. Life Sci.* 71, 683–697. <https://doi.org/10.1007/s00018-013-1459-1>
- Yip, V., Palma, E., Tesar, D.B., Mundo, E.E., Bumbaca, D., Torres, E.K., Reyes, N.A., Shen, B.Q., Fielder, P.J., Prabhu, S., Khawli, L.A., Boswell, C.A., 2014. Quantitative cumulative biodistribution of antibodies in mice: Effect of modulating binding affinity to the neonatal Fc receptor. *MAbs* 6, 689–696. <https://doi.org/10.4161/mabs.28254>
- Yu, J., Vodyanik, M.A., Smuga-Otto, K., Antosiewicz-Bourget, J., Frane, J.L., Tian, S., Nie, J., Jonsdottir, G.A., Ruotti, V., Stewart, R., Slukvin, I.I., Thomson, J.A., 2007. Induced pluripotent stem cell lines derived from human somatic cells. *Sci. (New York, NY)* 318, 1917–1920. <https://doi.org/10.1126/science.1151526>

**HIGHLIGHTS**

- iPSC-brain endothelial cells and NSC-astrocytes form an *in vitro* BBB model
- TNF- $\alpha$  and IL-6 cause BBB dysfunction via an increase in transcellular permeability
- With NSC-derived astrocytes, more proinflammatory cytokines are secreted
- Despite cytokines, NSC-astrocytes help barrier breakdown caused by TNF- $\alpha$  and IL-6
- This stem-cell derived BBB model can be used to understand disease progression